The European Journal of Biomedical and Life Sciences 2025, No 3
ISSN 2310-5674

PREMIER Publishing
ppublishing.org

Section 2. General biologi

DOI:10.29013/EJBLS-25-3-12-29

GITR AND TARGETED SMALL MOLECULES FOR CANCER IMMUNOTHERAPY

Vishresh Deepak [1]***, Dr. Moustafa Gabr*** [1]

[1] Weill Cornell Medicine College, New York, United States

Cite: *Vishresh Deepak, Moustafa Gabr. (2025). Gitr and Targeted Small Molecules For Cancer Immunotherapy. The European Journal of Biomedical and Life Sciences 2025, No. 3.* https://doi.org/10.29013/EJBLS-25-3-12-29

Abstract

While revolutionary cancer treatments see progress every day, cancer still remains a severe problem in our world. Immune checkpoint inhibitors, an advanced form of immunotherapy, is a treatment utilizing small molecules to override immune system checkpoints and enhance immune cell effector function. Glucocorticoid-induced TNFR-related (GITR) proteins are proteins expressed on various immune cells that can be activated to modulate cell function and impede immune cell suppression. Due to its potential role in enhancing immune system response to tumors, GITR and its ligand, GITRL, serve as strong potential drug targets for small molecules. This study aims to pre-clinically validate and screen GITR (and GITRL) as targets while identifying the most promising compounds for binding to the targets. The expensive, resource-dependent, and complex nature of drug discovery in research labs necessitates the need for a pre-clinical study. The research involves several computational methods to determine the feasibility of the target and compounds. The initial screening identifies possible binding sites on GITR and GITRL. Pharmacophore maps for GITR and GITRL were used to identify top molecular compounds for binding with GITR and GITRL. The energy of the compounds' interactions at the potential binding sites were analyzed using SwissDock. Using the top 5 compounds for GITR with highest predicted interaction energy, drug property evaluation (ADME potential and Lipinski's Rule validation) was conducted to further validate the compounds. The best compound for GITR was further evaluated to ensure safety and validity of compounds through toxicity prediction using ProTox 3.0. These computational methods result in the best compounds to be analyzed further clinically using both invivo and invitro methods. The results of this experiment streamline the initial screening of the targets and compounds as well as serve as the baseline for furthering immunotherapy techniques.

Keywords: *GITR, GITRL, cancer, immunotherapy, immune checkpoints, drug discovery*

1. Introduction

The physiological complexity of cancer creates the need for many different therapies and treatments. Major therapy areas such as chemotherapy and radiation therapy have been the standard for a while, while areas such as immunotherapy have been rising recently. Chemotherapy uses toxic drugs to kill cancerous tumors and mechanically affect the DNA to prevent cell division and replication (Li B., Shao H., Gao L., Li H., Sheng H., Zhu L., 2022; Wei G., Wang Y., Yang G., Wang Y., Ju R. 2021). Chemotherapy also inadvertently damages surrounding healthy cells and tissue (Li B., Shao H., Gao L., Li H., Sheng H., Zhu L., 2022). The limited efficacy of chemotherapy as well as the potential dangerous side effects caused by it create a need for a replacement treatment model (Chern Y. J., Tai I. T., 2020). Radiotherapy utilizes high doses of radiation to attack cancer cells and reduce tumor size. Like chemotherapy, radiotherapy also damages surrounding cells and creates side to healthy tissues (Chern Y. J., Tai I. T., 2020; Gong L., Zhang Y., Liu C., Zhang M., Han S., 2021). Immunotherapy strengthens and manipulates the immune cells to find and attack cancer cells. While it has minimal side effects, immunotherapy faces many limitations and blockades to effectively mitigate tumors. The major treatment modes are individually ineffective and have harmful side effects. The best method for cancer treatment consists of combination therapy techniques, utilizing several different techniques in conjunction (Bayat Mokhtari R., Homayouni T. S., Baluch N., Morgatskaya E., Kumar S., Das B., Yeger H., 2017).

Immunotherapy is a rapidly developing cancer treatment technique that stimulates the immune system to target and eliminate cancerous tumors (Tan S., Li D., Zhu X., 2020). Immunotherapy encompasses activating or modulating the immune cells to attack and regulate tumor cells. Through the improved natural defenses of the immune system, immune cells are able to penetrate the tumor microenvironment (TME) (Zhang Y., Zhang Z., 2020). The major primary activation methods of the immune cells include immune checkpoint inhibitors (ICIs), cancer vaccines, and CAR T-cell therapy. Immune checkpoints exist to prevent harm by an overly strong immune system to healthy cells. These checkpoints also prevent the immune cells from targeting and effectively attacking tumor cells, lowering immune cell function and response (Naimi A., Mohammed R. N., Raji A., Chupradit S., Yumashev A. V., Suksatan W., Shalaby M. N., Thangavelu L., Kamrava S., Shomali N., Sohrabi A. D., Adili A., Noroozi-Aghideh A., Razeghian E., 2022). ICIs, in the form of drugs, work by blocking checkpoint proteins from binding with partner proteins (such as tumor cell proteins), overriding the immune checkpoints (Papież M. A., Krzyściak W., 2021). Cancer vaccines utilize antigen based vaccines to reinvigorate the immune system to fight the cancer. During carcinogenesis, immune cells are blocked from penetrating the TME. The antigens administered by the vaccine are designed to replicate the tumor's antigens, allowing the immune cells to enter the TME and attack. the cancer cells (Cha J. H., Chan L. C., Song M. S., Hung M. C., 2020). CAR T-Cell therapy uses genetic modifications to personalize T-cells to fight specific cancer cells. The T-cells are modified by adding a chimeric antigen receptor (CAR), allowing the new CAR T-cell to search for and attack the specific cancer cells (Papież M. A., Krzyściak W. 2021). Each method of immune system activation addresses an individual hurdle of modulating the immune system. Every type of immunotherapy has its own advantages, offering a solution to a specific problem.

As immunotherapy is a developing treatment, there are several limitations and issues that arise when considering the specific therapy processes. Two of the largest limitations of immunotherapy are tumor resistance and immune cell exhaustion (Sterner R. C., Sterner R. M., 2021). Tumor resistance is the tumor's ability to resist or escape immune cell attacks and can take many forms. After being targeted by immune cells for a specific antigen expressed on the tumor, the tumor can display the loss of antigen expression, preventing immune cells from locating the tumor (Sterner R. C., Sterner R. M., 2021). Another method of tumor resistance is immune suppression, which uses the immune checkpoints to render immune cells ineffective. When the checkpoints are activated

by bonded antigens, the immune cell is disabled and the cell function is decreased (Burke K. P., Patterson D. G., Liang D., Sharpe A. H., 2023). Cell exhaustion is the condition of the cell with the effector function being reduced during interaction with tumor cells (Chow A., Perica K., Klebanoff C. A., Wolchok J. D., 2022). The repeated targeting of the antigen and attack on tumor lowers immune response efficacy and immune cell function while fighting cancer cells (Miggelbrink A. M., Jackson J. D., Lorrey S. J., Srinivasan E. S., Waibl-Polania J., Wilkinson D. S., Fecci P. E., 2021). These key issues pose limitations on the extent of immunotherapy to effectively fight cancer, and these limitations must be overcome to accomplish the potential of immunotherapy.

Figure 1. *Diagram displays GITR-immune checkpoint interaction (Knee D. A., Hewes B., Brogdon J. L., 2016)*

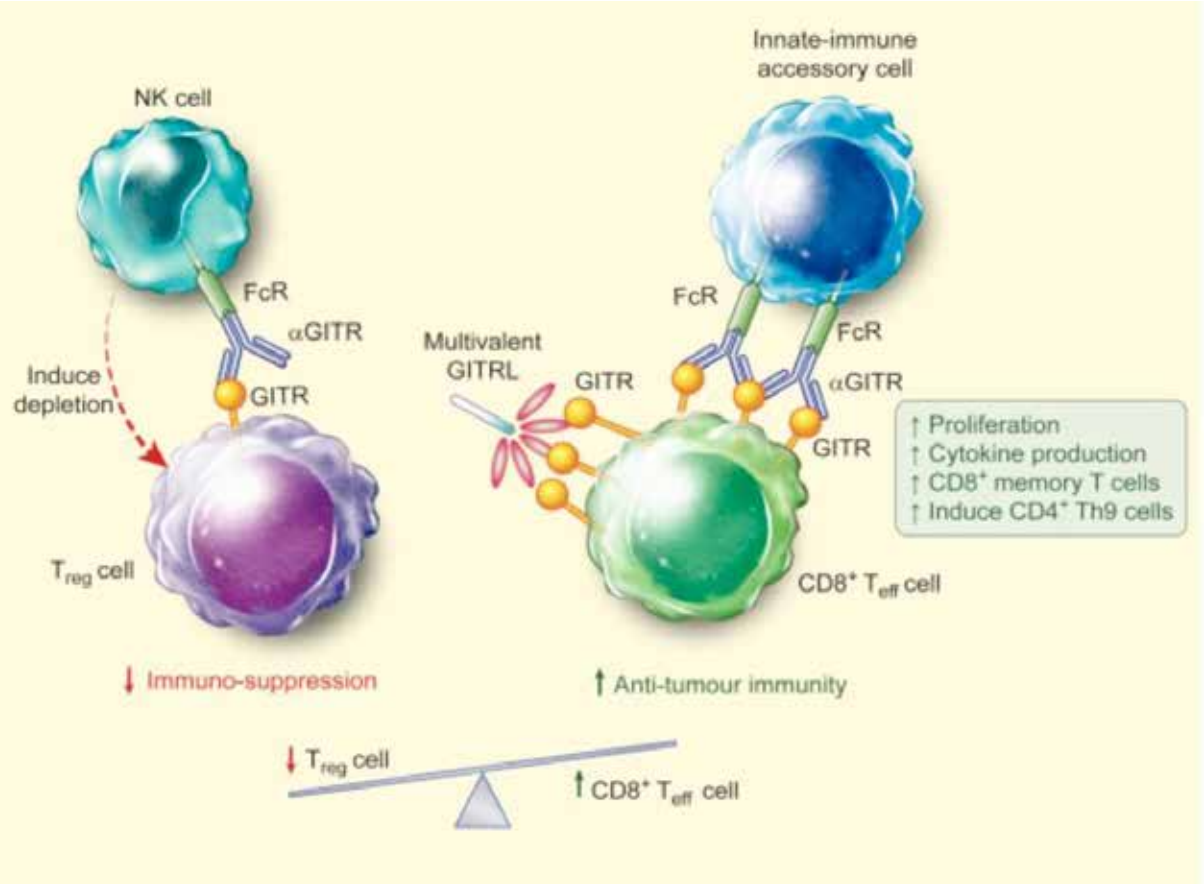

Glucocorticoid-induced TNFR-related (GITR) proteins are proteins that increase T-cell effector function and prevent regulatory T-cell function (Davar D., Zappasodi R., 2023). GITR proteins are part of the tumor necrosis factor receptor super-family (TNFRS), which are proteins that regulate immune cells (Buzzatti G., Dellepiane C., Del Mastro L., 2020). GITR becomes activated when bound with its ligand GITRL, which is most commonly found on antigen-presenting cells (APC), such as natural killer (NK) and regulatory (Treg) cells (Davar D., Zappasodi R., 2023; Buzzatti G., Dellepiane C., Del Mastro L., 2020; Krausz L. T., Bianchini R., Ronchetti S., Fettucciari K., Nocentini G., Riccardi C., 2007). GITR protein activation stimulates innate and acquired (adaptive) responses from the immune system (Davar D., Zappasodi R., 2023). Since immune cells have high expression of GITR and can increase function greatly after GITR activation, GITR has a high potential to be considered for creating a pathway for immunomodulation (Schaer D. A., Murphy J. T., Wolchok J. D., 2012). Utilizing GITR activation for an immunomodulation pathway

allows for the potential inhibition of immune checkpoints, a major step in cancer therapy.

Recent studies have shown promise in GITR's use in immune checkpoint inhibition methods. Studies such as Buzzat et al. 2020 (Buzzatti G., Dellepiane C., Del Mastro L., 2020) have proved GITR's feasibility in serving as a co-stimulatory agent, while lacking efficiency as a monotherapy. The results indicate promise in combination therapy involving GITR while prompting the need for clinical studies to validate this. Other studies such as Zappasodi et al. (Zappasodi R., Sirard C., Li Y., Budhu S., Abu-Akeel M., Liu C., Yang X., Zhong H., Newman W., Qi J., Wong P., Schaer D., Koon H., Velcheti V., Hellmann M. D., Postow M. A., Callahan M. K., Wolchok J. D., Merghoub T., 2019) have shown using in vivo experiments with mice that GITR work can work well in monotherapies with limited assistance from other factors such as cell reinvigoration.

2. Methodology

2.1 Binding Site Identification

There are several methods used to identify potential binding sites, the main ones being geometric, energetic, machine learning, and template-based. Our research consists of utilizing only the first three methods using the resources of Proteins Plus DoGSite Scorer, BU EDU FTSite, and P2Rank PrankWeb.

2.1.1 DoGSiteScorer

DoGSiteScorer (https://proteins.plus) is a tool analyzing the geometric element of binding sites. It uses a Difference of Gaussian filter to identify potential binding sites based on the 3d structure of the protein (Schöning-Stierand, K., Diedrich, K., Ehrt, C., Flachsenberg, F., Graef, J., Sieg, J., Penner, P., Poppinga, M., Ungethüm, A., Rarey, M., 2022). DoGSiteScorer uses geometric methods to identify regions on the given protein geometrically suitable (eg. volume) for binding to small molecules. DoGSiteScorer provides possible binding sites, their drug scores, and geometric data such as volume and surface areas.

Using the PDB code '7KHD', enter the code into the Proteins Plus server main page. Select the DoGSiteScorer tool and select the desired chains (A and B for GITRL and C and D for GITR). The calculation results in a diagram of geometrically suitable binding sites with surface area and volume information about each binding site as well as a drug score (out of 1).

2.1.2 FT Site

FT Site (https://ftsite.bu.edu) is a tool to analyze potential binding sites based on the energy of the site. FT Site calculates the polarities and energy requirements of the elements to search and identify potential binding sites on the protein (Kozakov D., Grove L. E., Hall D. R., Bohnuud T., Mottarella S. E., Luo L., Xia B., Beglov D., Vajda S., 2015; Ngan C. H., Hall D. R., Zerbe B. S., Grove L. E., Kozakov D., Vajda S., 2012; Brenke R., Kozakov D., Chuang G. Y., Beglov D., Hall D., Landon M. R., Mattos C., Vajda S., 2009). FT Site identifies binding sites with balanced polarities and required interaction energy.

Use Boston University's FT Site Server by entering the PDB code '7KHD'. Run the prediction simulation once for GITRL by entering "A B"' for chain ids and another time for GITR by entering "C D" for chain ids. The result of the simulation will provide a diagram of the protein structure with highlighted regions for possible binding sites.

2.1.3 PrankWeb

PrankWeb (https://prankweb.cz) uses machine learning to identify binding sites based on a variety of factors together. It uses algorithms to identify the best possible intersections of factors such as polarity balance to ensure optimal binding site conditions (Dávid Jakubec, Petr Škoda, Radoslav Krivák, Marian Novotný and David Hoksza. 2022; Lukáš Jendele and Radoslav Krivák and Petr Škoda and Marian Novotný and David Hoksza. 2019; Radoslav Krivák and David Hoksza. 2018).

Enter the PDB code '7KHD' into PrankWeb. Uncheck the original structure box, select all 4 chains, and submit the query. The results will provide a diagram of protein structure and amino acids with highlighted regions for each binding site. A table with each binding pocket provides information about the overall score (out of 10), the probability of binding with compounds, and number of residues (amino acids) making up the pocket.

2.2 Pharmacophore Virtual Screening

PocketQuery (http://pocketquery.csb.pitt.edu/) is a web service analyzing protein-protein interactions and providing information about the clusters and residues. It provides metrics such as size of clusters, energy scores, and best cluster matches. Pocketquery provides pharmacophore maps to map interaction between proteins.

Enter the PDB code '5skh9' into PocketQuery and submit the query. The results of the query will provide a list of the top clusters for the given query. A table provides information on the number of residues, distance, Gibbs free energy and Rosetta energy values, solvent accessible surface area information for each cluster.

2.3 Compound Virtual Screening

ZincPharmer (http://zincpharmer.csb.pitt.edu/pharmer.html) is a tool and database of different compounds used to identify potential compounds for binding pockets identified using PocketQuery.

Once the selected cluster is sent to ZincPharmer, the results will be displayed in the form of a table with compounds that have similar matches to bond. The lowest RMSD scores are the best compounds to bind. The table provides RMSD (deviation score), compound mass, and amino acid count.

2.4 Compound Virtual Molecular Docking

SwissDock (https://www.swissdock.ch/) is a virtual tool to analyze the energy interaction between each compound and protein. The energy of the interactions between the protein and the compound are shown in a table. Each interaction has a SwissParam score, an estimate of the binding interaction's free energy as a weighted sum of the polar and nonpolar terms, and the AC (Attracting cavities) score, the combined score of the CHARMM (Chemistry at Harvard Macromolecular Mechanics) force field energy (potential energy at atomic scale), and the FACTS (Fast Analytical Continuum Treatment of Solvation) solvation energy.

Enter in the SMILES id from the Zinc database for each compound. Enter PDB code '7khd' for the target and prepare the target. Increase the size bounds to fit that target. Select one parameter, click check parameters, and submit the query.

2.5 Drug Property and Likeness Evaluation

SwissADME (http://www.swissadme.ch/) is a tool to determine and verify the drug properties of the selected compounds. SwissADME uses compound properties to analyze whether the compound is a suitable drug by checking against rules such as Lipinski's rule. It also checks a variety of other factors that can be chosen.

Enter the SMILES id from the Zinc database and run the tool. A table of property values, property levels, and present factors are provided for each compound.

2.6 Compound Toxicity Prediction

ProTox 3.0 (https://tox.charite.de/protox3/index.php?site=compound_input) is a tool to analyze the safety and toxicity of the compounds with the human body. It compares the toxic components with average FDA approved compounds and identifies active toxic components.

Enter the SMILES id from the Zinc database or the compound name. Select all the factors and run the simulation. The LD50 and toxicity class will be reported as well as diagrams of the toxicity factors and levels.

3. Results

3.1 GITR Binding Sites

The results of the 3 binding site discovery methods are shown below to indicate the potential of small molecules binding to GITR.

3.1.1 DoGSiteScorer

DoGSiteScorer identified 5 potential binding pockets across GITR chains C and D and identified 10 potential binding pockets across GITRL chains A and B. Tables 1 and 2 detail the volume, surface area, and drug score (out of 1) about each possible pocket shown in Figure 2 (below). GITR (Chains C and D) had 5 total possible pockets while GITRL (chains A and B) had 10 total possible pockets. While GITRL was identified as having more potential pockets, GITR pockets had significantly higher high scores (0.78 and 0.74) than the highest high scores of GITRL pockets.

The GITR pocket with the highest drug score is P_0 on chain C, with a score of 0.78. This pocket also has the largest volume, 580.74 $Å^3$, and surface area, 960.32

Å². The data indicates pocket P_0 is the most prominent for binding to GITR. The GITRL pocket with the highest drug score is P_1 on chain A, with a drug score of 0.56. The pocket has a volume of 168.19 Å³ and surface area of 253.05 Å². It has a relatively lower drug score, volume, and surface area, indicating GITR has a better binding site in terms of binding chance.

Additionally, GITR has a higher average pocket drug score, with an average score of 0.49, than GITRL, with an average score of 0.332. GITRL has a notable similarity between each of its pockets, with similarly ranging drug scores and volumes. This consistency indicates low variation amongst the pockets, lowering the chances of binding to GITRL.

Table 1. *Table with found pockets and relevant data for binding sites to GITR*

Chain C:				
Diagram Color	**Site Number**	**Volume**	**Surface Area**	**Drug Score**
Yellow	P_0	580.74 Å³	960.32 Å²	0.78
Purple	P_1	128.58 Å³	331.07 Å²	0.29
Chain D:				
Diagram Color	**Site Number**	**Volume**	**Surface Area**	**Drug Score**
Yellow	P_0	494.02 Å³	650.4 Å²	0.74
Purple	P_1	193.79 Å³	349.29 Å²	0.43
Green	P_2	103.94 Å³	263.07 Å²	0.21

Table 2. *Table with found pockets and relevant data for binding sites to GITRL*

Chain A:				
Diagram Color	**Site Number**	**Volume**	**Surface Area**	**Drug Score**
Yellow	P_0	216.32 Å³	468.31 Å²	0.35
Purple	P_1	168.19 Å³	253.05 Å²	0.56
Green	P_2	156.93 Å³	439.62 Å²	0.28
Red	P_3	133.44 Å³	253.27 Å²	0.32
Blue	P_4	105.41 Å³	99.03 Å²	0.23
Chain B:				
Diagram Color	**Site Number**	**Volume**	**Surface Area**	**Drug Score**
Yellow	P_0	165.7 Å³	304.43 Å²	0.5
Purple	P_1	145.02 Å³	294.36 Å²	0.3
Green	P_2	111.3 Å³	198.4 Å²	0.22
Red	P_3	106.88 Å³	146.07 Å²	0.37
Blue	P_4	105.41 Å³	105.5 Å²	0.19

Figure 2. *Displays the DoGSiteScorer predicted binding sites on the chains of GITR and GITRL highlighted by the neon colored regions*

Chain C (GITR)

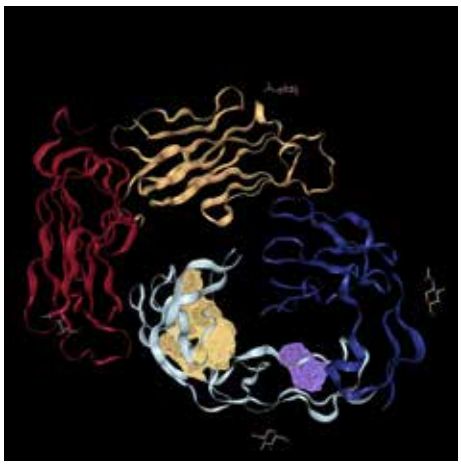

Chain D (GITR)

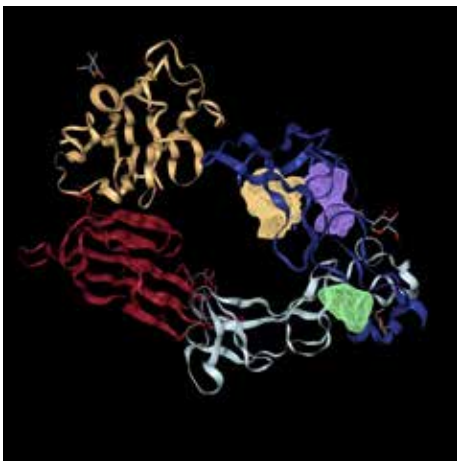

Chain A (GITRL)

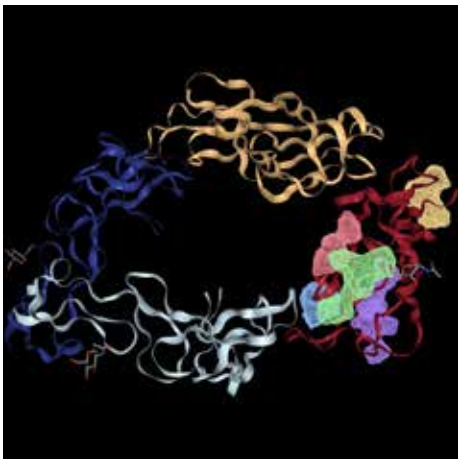

Chain B (GITRL)

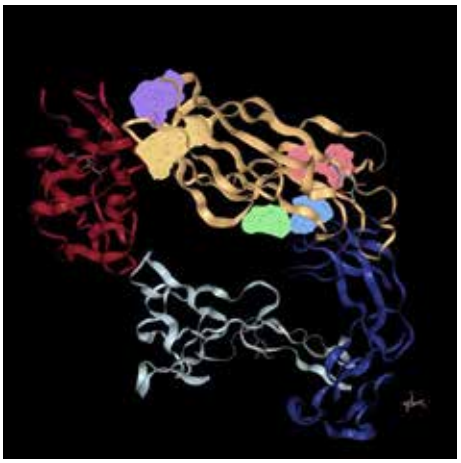

3.1.2 FTSite:

FTSite found 3 binding sites on both GITR and GITRL shown below based on interaction energy at potential binding sites.

Figure 3. *Displays the FTSite predicted binding sites of GITR and GITRL highlighted by the red, purple, and green regions*

GITR Binding Sites

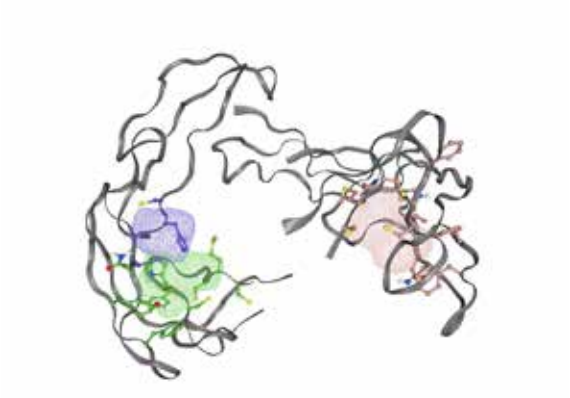

GITRL Binding Sites

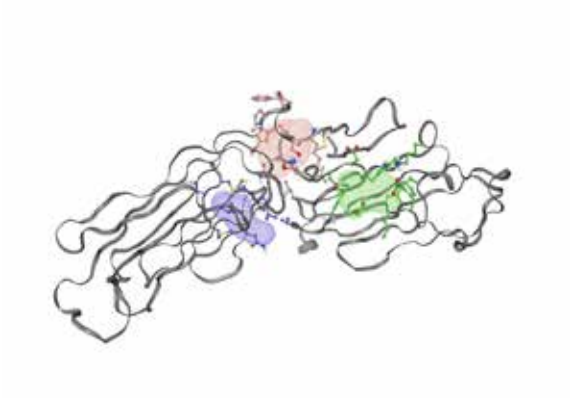

3.1.3 PrankWeb:

PrankWeb identified 9 possible binding sites, 4 on GITR (chains C and D) and 5 on GITRL (chains A and B). Tables 3 and 4 show the pocket score (out of 10), probability of successful binding (out of 1), and the residues, or amino acids, that make up each pocket.

Table 3. *GITR Binding Site Details*

Diagram Color	Pocket Number	Score	Probability	# of Residues
Green	5	2.81	0.088	9
Dark Blue	6	2.12	0.048	12
Pink	7	1.47	0.020	6
Camo Green	9	0.89	0.009	7

Table 4. *GITRL Binding Site Details*

Diagram Color	Pocket Number	Score	Probability	# of Residues
Red	1	4.82	0.225	12
Yellow	2	3.99	0.168	13
Orange	3	3.64	0.142	7
Blue	4	3.26	0.117	9
Dark Pink	8	1.11	0.004	8

Figure 4. *Identified Binding Pockets in GITR and GITRL (PDB ID: 7KHD) using Prankweb*

GITR (Pockets 5 and 9)

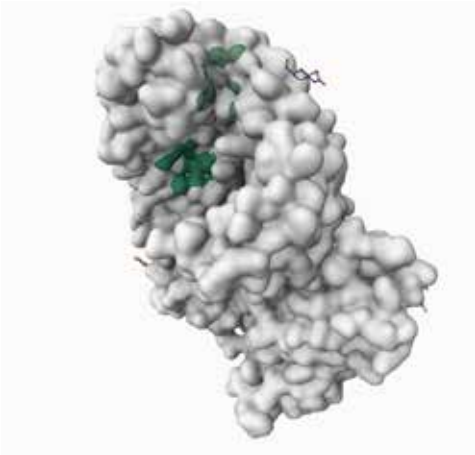

GITR (Pockets 6 and 7)

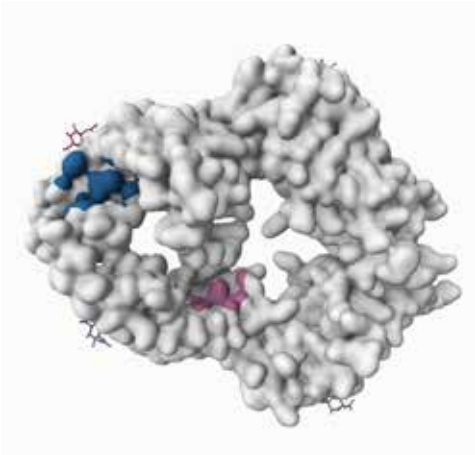

GITRL (Pocket 1)

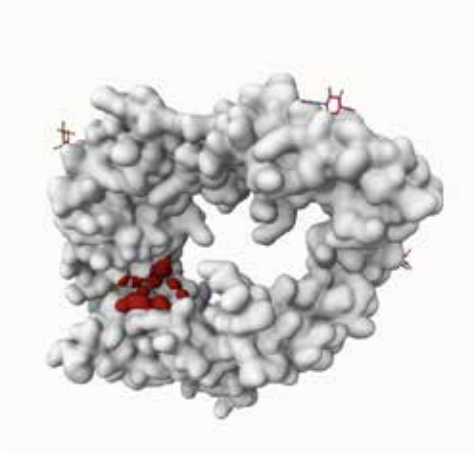

GITRL (Pockets 2, 3, 4, 8)

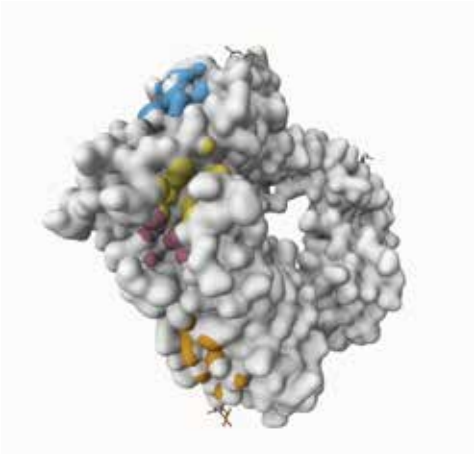

All the potential binding pockets for GITR had relatively low pocket scores and probabilities. Of these, pocket 5 had the most potential with a score of 2.81 and a probability of 0.088 (8.8% chance to successfully bind). Potential binding pockets for GITRL showed significantly more promising results. The most promising of these was pocket 1, with a score of 4.82 and a probability of 0.225 (22.5% chance to successfully bind). GITRL's potential binding sites had better results, with better average scores and probabilities.

3.2 Pharmacophore Virtual Screening

The top 20 compounds for binding to both GITR and GITRL are shown below in tables 5 and 6. Potential compounds for GITRL binding showed significantly lower (between 4 to 8 times lower) deviation scores (RMSD) than GITR, indicating less difference between the perfect binding molecules and the potential compounds. Figures 5 and 6 below depict the overlay between the ideal pharmacophore maps and compound diagrams.

Table 5. *ZincPharmer compounds of best 20 compounds with least pharmacophore map and compound structure overlay deviation according to PocketQuery for binding to GITR*

Compound	RMSD	Mass	RBnds
ZINC14199378	0.013	418	5
ZINC09633628	0.013	442	7
ZINC12921150	0.013	429	5
ZINC09548422	0.014	403	5
ZINC03357714	0.014	460	6
ZINC08882059	0.015	327	6
ZINC08882818	0.015	438	5
ZINC09366332	0.015	446	7
ZINC02405966	0.016	471	7
ZINC91672374	0.016	266	3
ZINC78563990	0.008	332	10
ZINC13775229	0.016	493	6
ZINC24834540	0.016	429	10
ZINC32901681	0.017	481	8
ZINC20808334	0.017	432	4
ZINC03387454	0.018	448	5
ZINC19559453	0.018	283	5
ZINC00545907	0.019	306	0
ZINC90064795	0.020	315	2
ZINC09548119	0.020	396	4

Figure 5. *ZincPharmer compound structure diagrams of pharmacophore map and compound structure overlay of best 20 compounds with least deviation according to PocketQuery for binding to GITR*

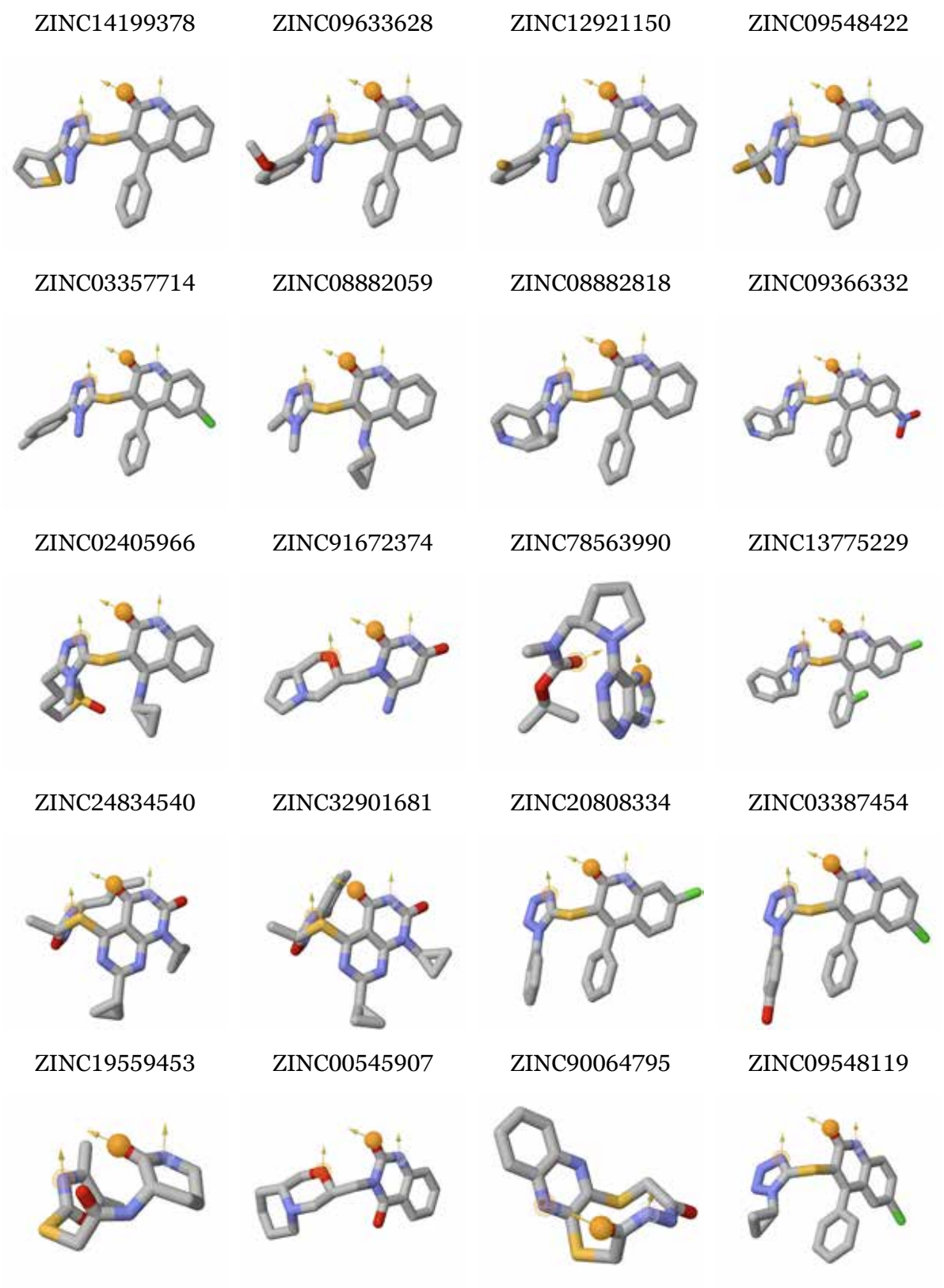

Table 6. *ZincPharmer compounds of best 20 compounds with least pharmacophore map and compound structure overlay deviation according to PocketQuery for binding to GITRL*

Compound	RMSD	Mass	RBnds
ZINC15722443	0.002	432	6
ZINC71846525	0.002	479	13
ZINC09830796	0.003	472	8
ZINC28649737	0.003	379	6
ZINC38845794	0.003	433	12
ZINC94231157	0.003	325	7
ZINC31365432	0.003	431	11
ZINC09336512	0.003	437	8
ZINC33523946	0.003	424	7
ZINC77642707	0.003	297	6
ZINC05676781	0.003	317	4
ZINC32529877	0.003	488	13
ZINC92926086	0.004	274	5
ZINC80435793	0.004	338	8
ZINC00902385	0.004	453	7
ZINC12556729	0.004	471	8
ZINC92941172	0.004	274	5
ZINC57321987	0.004	223	9
ZINC90393652	0.004	310	8
ZINC32528815	0.004	472	12

Figure 6. *ZincPharmer compound structure diagrams of pharmacophore map and compound structure overlay of best 20 compounds with least deviation according to PocketQuery for binding to GITRL*

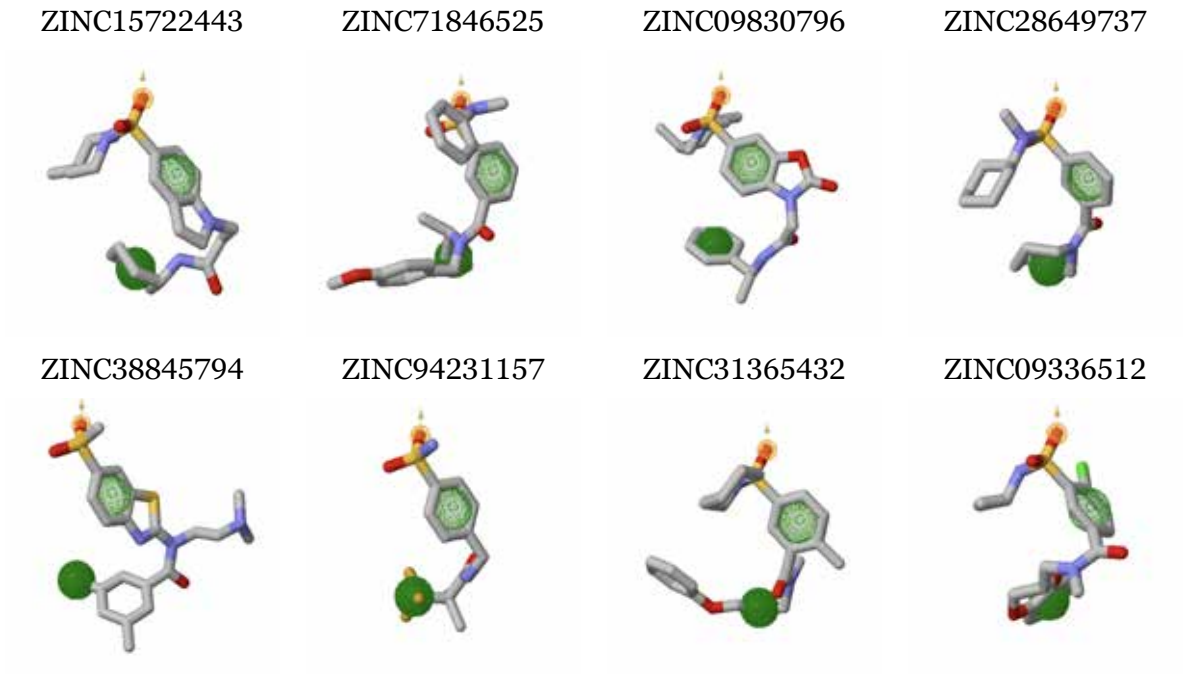

714

ZINC33523946 ZINC77642707 ZINC05676781 ZINC32529877

ZINC92926086 ZINC80435793 ZINC00902385 ZINC12556729

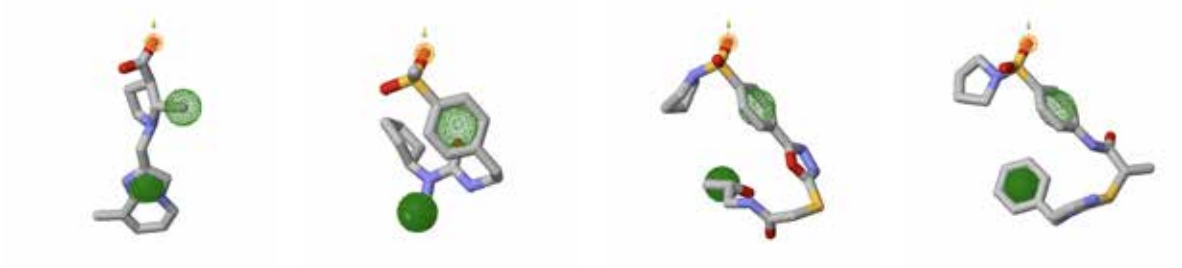

ZINC92941172 ZINC57321987 ZINC90393652 ZINC32528815

3.3 SwissDock Energy Interaction Results

Table 7. *SwissDock scores for binding site energy interaction for GITR*

Compound Name	AC Score	SwissParam Score
ZINC14199378	42.055227	−7.7650
ZINC09633628	58.893459	−7.8380
ZINC12921150	52.017029	−7.7460
ZINC09548422	16.941301	−7.2330
ZINC03357714	50.282898	−7.5979
ZINC08882059	202.679021	−7.3255
ZINC08882818	254.268250	−7.5837
ZINC09366332	199.002316	−7.9039
ZINC02405966	32.049053	−7.6664
ZINC91672374	−97.437807	−6.5076
ZINC78563990	−12.333222	−7.1619
ZINC13775229	20.172356	−7.6213
ZINC24834540	317.305069	−7.4686
ZINC32901681	342.057852	−7.8020

Compound Name	AC Score	SwissParam Score
ZINC14199378	42.055227	–7.7650
ZINC09633628	58.893459	–7.8380
ZINC12921150	52.017029	–7.7460
ZINC09548422	16.941301	–7.2330
ZINC03357714	50.282898	–7.5979
ZINC08882059	202.679021	–7.3255
ZINC08882818	254.268250	–7.5837
ZINC09366332	199.002316	–7.9039
ZINC02405966	32.049053	–7.6664
ZINC91672374	–97.437807	–6.5076
ZINC78563990	–12.333222	–7.1619
ZINC20808334	41.970624	–7.6083
ZINC03387454	30.239117	–7.9282
ZINC19559453	–20.043652	–7.3410
ZINC00545907	79.767973	–6.9247
ZINC90064795	–39.183751	–6.7137
ZINC09548119	244.290199	–7.4288

Figure 7. *SwissDocks's highest energy interaction diagram for binding to each identified compound shown above*

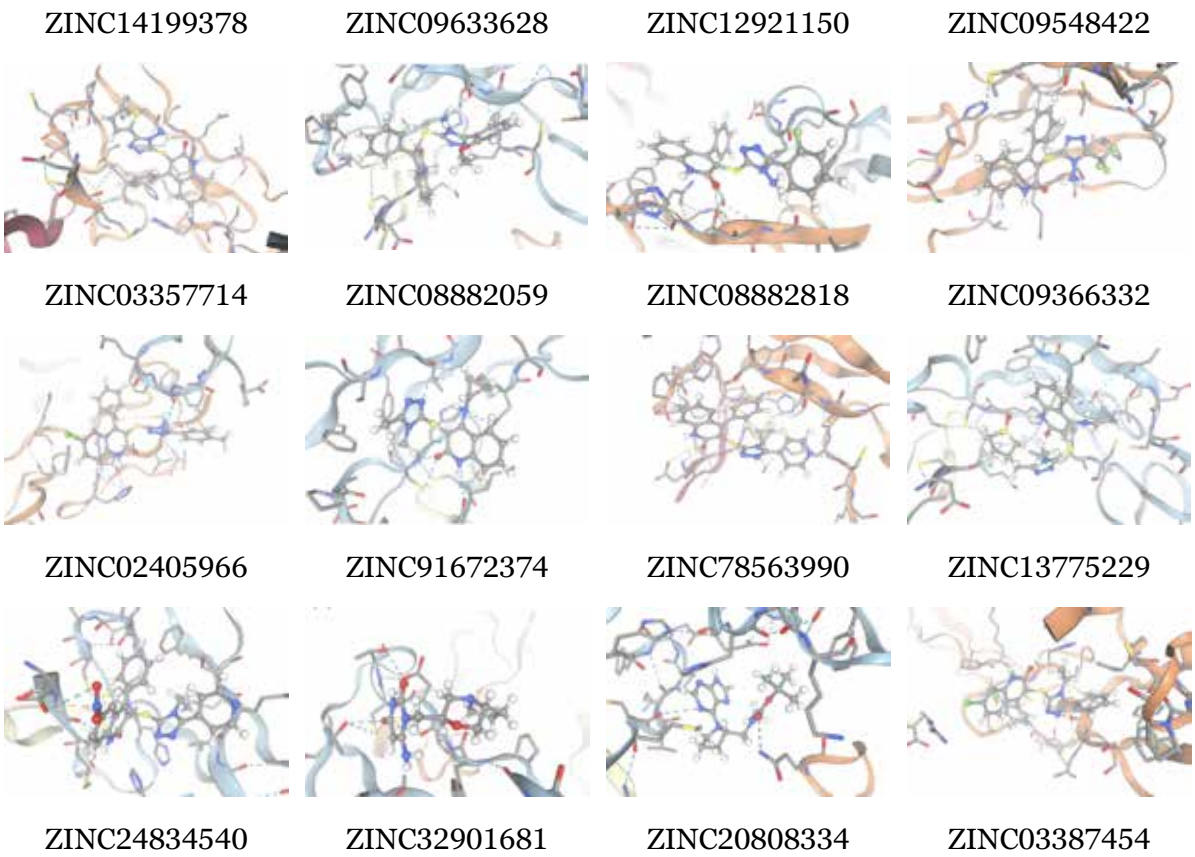

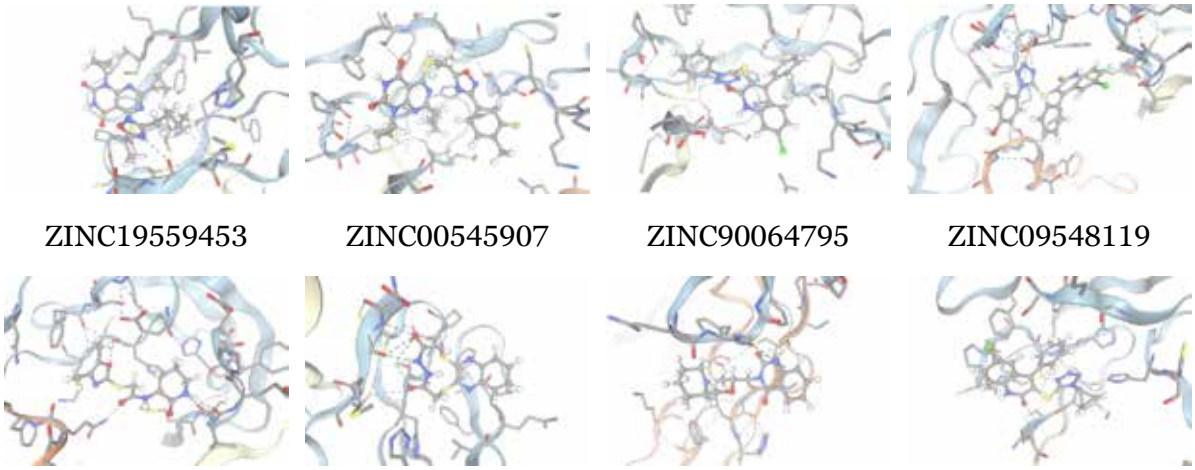

ZINC19559453 ZINC00545907 ZINC90064795 ZINC09548119

3.4 Swiss ADME Drug Evaluation

The SwissADME druglikeness evaluation used the five compounds with the highest energy interaction at the binding sites. The compounds (shown in tables 6 and 7) were tested to evaluate the attributes shown below. All 5 compounds passed Lipinski's rule evaluation with zero violations. The compounds all had similar attributes for GI absorption and BBB permeant. However, ZINC09366332 had a notably higher solubility than the other compounds.

Table 6. *Lipinski's Rule evaluation of top 5 identified compounds*

Compound	Number of Hydrogen Bond Donors	Number of Hydrogen Bond Acceptors	Calculated LogP (CLogP) Value	Molecular Mass (in Daltons)
ZINC14199378	2	3	2.79	417.51
ZINC09633628	2	4	3.43	441.50
ZINC09366332	2	5	1.84	445.56
ZINC32901681	1	8	3.73	480.51
ZINC03387454	2	5	3.03	447.90

Table 7. *Additional Attribute Evaluation*

Compound	Water Solubility (mg/ml)	Water Solubility Classification	Gastrointestinal (GI) Absorption	Blood Brain Barrier (BBB) Permeant
ZINC14199378	2.65×10^{-3}	Moderately Soluble	Low	No
ZINC09633628	1.77×10^{-3}	Moderately Soluble	Low	No
ZINC09366332	9.06×10^{-2}	Soluble	Low	No
ZINC32901681	4.01×10^{-3}	Moderately Soluble	Low	No
ZINC03387454	4.93×10^{-4}	Moderately Soluble	Low	No

3.5 ProTox Drug Toxicity Evaluation

Protox 3.0 showed that the top compound, ZINC09366332, had a LD50 of 160 mg/kg and predicted toxicity class of 3 (1 being the most toxic). Additionally, the key toxicity factors are shown below. The compound's toxicity was compared to the average toxicity of FDA approved drugs shown in Figure 8. The active toxic components are shown in Figure 9.

Figure 8. *Comparison of toxicity factors in Kinetin (most similar compound to ZINC09366332), to average toxicity of FDA approved compounds*

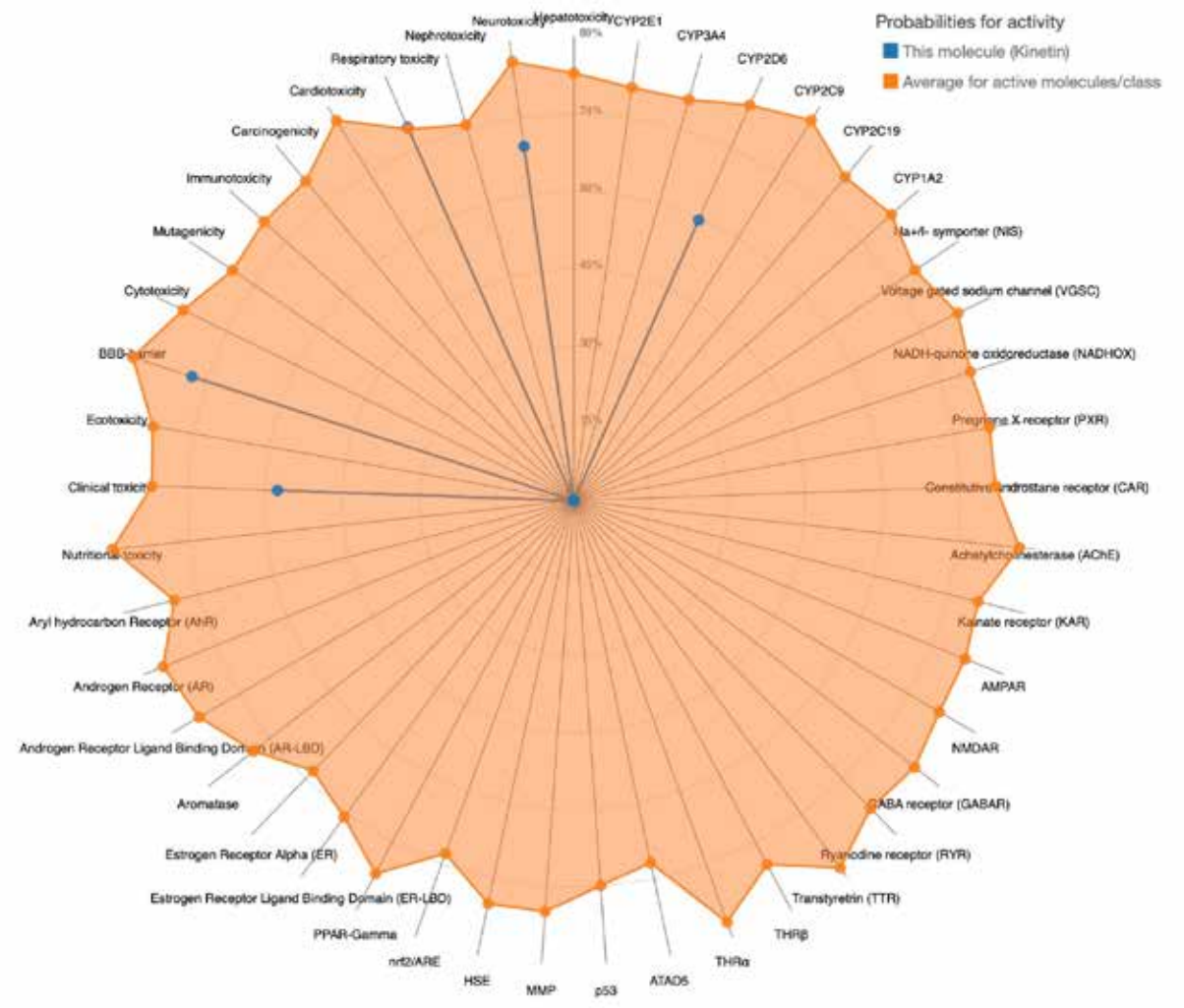

Figure 9. *Shows the active and inactive toxic components of Kinetin (closest compound to ZINC09366332)*

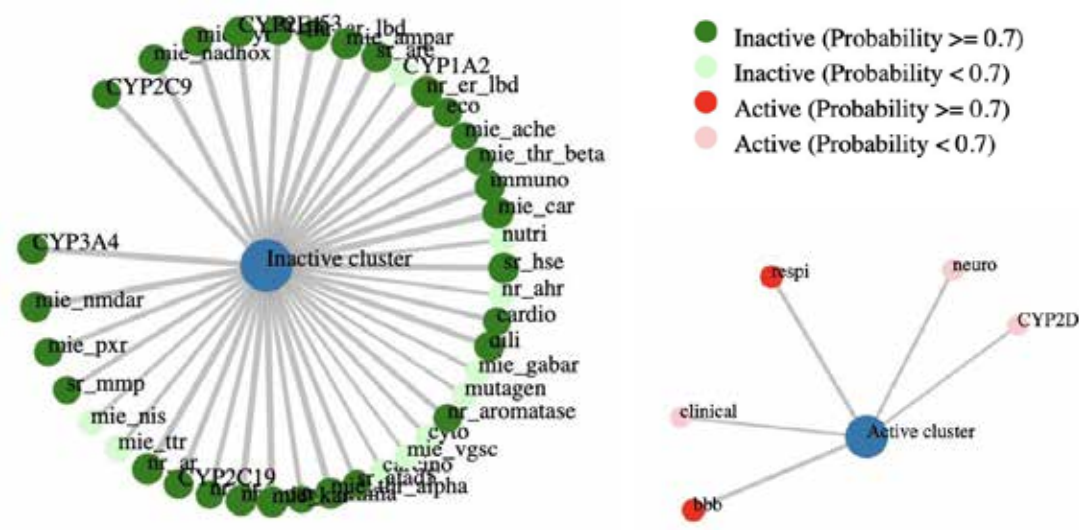

Kinetin

4. Conclusion

Being one of the most dangerous and deadly conditions, cancer requires constant innovation to combat. Improving and advancing the newest therapies are one of the most effective ways to continue this. With immunotherapy being the best rising treatment, enhancing its ability is crucial to its success. This study aims to elevate immunotherapy by providing a basis for advancing the therapy through small molecule immunomodulation. Initial testing showed binding to GITR has a high potential. Further screening of the binding sites and potential compounds shows promise in finding compounds that bind to GITR. Compound interaction energies are high enough to bind properly. Through this workflow ZINC09366332 was shown to have the most promise in successfully binding to GITR. Drug property and toxicity testing further proved the ability of ZINC09366332 to be a strong compound. However, clinical studies are necessary to fully prove the feasibility of this interaction and compound. Initial research also showed GITRL is a viable target for compound binding and should also be evaluated to advance the therapy.

References

Li B., Shao H., Gao L., Li H., Sheng H., Zhu L. Nano-drug co-delivery system of natural active ingredients and chemotherapy drugs for cancer treatment: a review. Drug Deliv. 2022 Dec; 29(1): 2130–2161. Doi: 10.1080/10717544.2022.2094498. Erratum in: Drug Deliv. 2022 Dec;29(1):3051. Doi: 10.1080/10717544.2022.2127213. PMID: 35815678; PMCID: PMC9275501. https://www.ncbi.nlm.nih.gov/pmc/articles/PMC9275501/pdf/IDRD_29_2094498.pdf

Wei G., Wang Y., Yang G., Wang Y., Ju R. Recent progress in nanomedicine for enhanced cancer chemotherapy. Theranostics. 2021 Apr 19; 11(13): 6370–6392. Doi: 10.7150/thno.57828. PMID: 33995663; PMCID: PMC8120226. https://www.ncbi.nlm.nih.gov/pmc/articles/PMC8120226/pdf/thnov11p6370.pdf

Chern Y. J., Tai I. T. Adaptive response of resistant cancer cells to chemotherapy. Cancer Biol Med. 2020 Nov 15; 17(4): 842–863. Doi: 10.20892/j.issn.2095–3941.2020.0005. Epub 2020 Dec 15. PMID: 33299639; PMCID: PMC7721100. https://www.ncbi.nlm.nih.gov/pmc/articles/PMC7721100/pdf/cbm-17-842.pdf

Gong L., Zhang Y., Liu C., Zhang M., Han S. Application of Radiosensitizers in Cancer Radiotherapy. Int J Nanomedicine. 2021 Feb 12; 16: 1083–1102. Doi: 10.2147/IJN.S290438. Erratum in: Int J Nanomedicine. 2021 Dec 16; 16: 8139–8140. Doi: 10.2147/IJN.S352169. PMID: 33603370; PMCID: PMC7886779. https://www.ncbi.nlm.nih.gov/pmc/articles/PMC7886779/pdf/ijn-16-1083.pdf

Bayat Mokhtari R., Homayouni T. S., Baluch N., Morgatskaya E., Kumar S., Das B., Yeger H. Combination therapy in combating cancer. Oncotarget. 2017 Jun 6; 8(23): 38022–38043. Doi: 10.18632/oncotarget.16723. PMID: 28410237; PMCID: PMC5514969. https://www.ncbi.nlm.nih.gov/pmc/articles/PMC5514969/pdf/oncotarget-08-38022.pdf

Tan S., Li D., Zhu X. Cancer immunotherapy: Pros, cons and beyond. Biomed Pharmacother. 2020 Apr; 124: 109821. Doi: 10.1016/j.biopha.2020.109821. Epub 2020 Jan 18. PMID: 31962285. https://www.sciencedirect.com/science/article/pii/S0753332220300111?ref=pdf_download&fr=RR-2&rr=994a848bcfbeec39

Zhang Y., Zhang Z. The history and advances in cancer immunotherapy: understanding the characteristics of tumor-infiltrating immune cells and their therapeutic implications. Cell Mol Immunol. 2020 Aug; 17(8): 807–821. Doi: 10.1038/s41423–020–0488–6. Epub 2020 Jul 1. PMID: 32612154; PMCID: PMC7395159. https://www.ncbi.nlm.nih.gov/pmc/articles/PMC7395159/pdf/41423_2020_Article_488.pdf

Naimi A., Mohammed R. N., Raji A., Chupradit S., Yumashev A. V., Suksatan W., Shalaby M. N., Thangavelu L., Kamrava S., Shomali N., Sohrabi A. D., Adili A., Noroozi-Aghideh A., Razeghian E. Tumor immunotherapies by immune checkpoint inhibitors (ICIs); the pros and cons. Cell Commun Signal. 2022 Apr 7; 20(1): 44. Doi: 10.1186/s12964–022–00854-y.

PMID: 35392976; PMCID: PMC8991803. https://www.ncbi.nlm.nih.gov/pmc/articles/PMC8991803/pdf/12964_2022_Article_854.pdf

Papież M. A., Krzyściak W. Biological Therapies in the Treatment of Cancer-Update and New Directions. Int J Mol Sci. 2021 Oct 28; 22(21): 11694. Doi: 10.3390/ijms222111694. PMID: 34769123; PMCID: PMC8583892. https://www.ncbi.nlm.nih.gov/pmc/articles/PMC8583892/pdf/ijms-22-11694.pdf

Cha J. H., Chan L. C., Song M. S., Hung M. C. New Approaches on Cancer Immunotherapy. Cold Spring Harb Perspect Med. 2020 Aug 3;10(8): a036863. Doi: 10.1101/cshperspect.a036863. PMID: 31615865; PMCID: PMC7156317. https://www.ncbi.nlm.nih.gov/pmc/articles/PMC7156317/pdf/cshperspectmed-MET-a036863.pdf

Sterner R. C., Sterner R. M. CAR-T cell therapy: current limitations and potential strategies. Blood Cancer J. 2021 Apr 6; 11(4): 69. Doi: 10.1038/s41408–021–00459–7. PMID: 33824268; PMCID: PMC8024391. https://www.ncbi.nlm.nih.gov/pmc/articles/PMC8024391/pdf/41408_2021_Article_459.pdf

Burke K. P., Patterson D. G., Liang D., Sharpe A. H. Immune checkpoint receptors in autoimmunity. Curr Opin Immunol. 2023 Feb; 80: 102283. Doi: 10.1016/j.coi.2023.102283. Epub 2023 Jan 28. PMID: 36709596; PMCID: PMC10019320. https://www.ncbi.nlm.nih.gov/pmc/articles/PMC10019320/pdf/nihms-1864696.pdf

Chow A., Perica K., Klebanoff C. A., Wolchok J. D. Clinical implications of T cell exhaustion for cancer immunotherapy. Nat Rev Clin Oncol. 2022 Dec; 19(12): 775–790. Doi: 10.1038/s41571–022–00689-z. Epub 2022 Oct 10. PMID: 36216928; PMCID: PMC10984554. https://www.ncbi.nlm.nih.gov/pmc/articles/PMC10984554/pdf/nihms-1972926.pdf

Miggelbrink A. M., Jackson J. D., Lorrey S. J., Srinivasan E. S., Waibl-Polania J., Wilkinson D. S., Fecci P. E. CD4 T-Cell Exhaustion: Does It Exist and What Are Its Roles in Cancer? Clin Cancer Res. 2021 Nov 1; 27(21): 5742–5752. Doi: 10.1158/1078–0432.CCR-21–0206. Epub 2021 Jun 14. PMID: 34127507; PMCID: PMC8563372. https://www.ncbi.nlm.nih.gov/pmc/articles/PMC8563372/pdf/5742.pdf

Davar D., Zappasodi R. Targeting GITR in cancer immunotherapy – there is no perfect knowledge. Oncotarget. 2023 Jun 19; 14: 614–621. Doi: 10.18632/oncotarget.28461. PMID: 37335294; PMCID: PMC10278658. https://www.ncbi.nlm.nih.gov/pmc/articles/PMC10278658/pdf/oncotarget-14-28461.pdf

Buzzatti G., Dellepiane C., Del Mastro L. New emerging targets in cancer immunotherapy: the role of GITR. ESMO Open. 2020 Aug; 4(Suppl 3): e000738. Doi: 10.1136/esmoopen-2020–000738. PMID: 32817129; PMCID: PMC7451269. https://www.ncbi.nlm.nih.gov/pmc/articles/PMC7451269/pdf/esmoopen-2020-000738.pdf

Krausz L. T., Bianchini R., Ronchetti S., Fettucciari K., Nocentini G., Riccardi C. GITR-GITRL system, a novel player in shock and inflammation. ScientificWorldJournal. 2007 May 1; 7: 533–66. Doi: 10.1100/tsw.2007.106. PMID: 17525820; PMCID: PMC5901298. https://www.ncbi.nlm.nih.gov/pmc/articles/PMC5901298/pdf/TSWJ-2007-7-738254.pdf

Nocentini G., Ronchetti S., Cuzzocrea S., Riccardi C. GITR/GITRL: more than an effector T cell co-stimulatory system. Eur J Immunol. 2007 May; 37(5): 1165–9. Doi: 10.1002/eji.200636933. PMID: 17407102. https://onlinelibrary.wiley.com/doi/epdf/10.1002/eji.200636933

Schaer D. A., Murphy J. T., Wolchok J. D. Modulation of GITR for cancer immunotherapy. Curr Opin Immunol. 2012 Apr; 24(2): 217–24. Doi: 10.1016/j.coi.2011.12.011. Epub 2012 Jan 12. PMID: 22245556; PMCID: PMC3413251. https://www.ncbi.nlm.nih.gov/pmc/articles/PMC3413251/pdf/nihms347224.pdf

Knee D. A., Hewes B., Brogdon J. L. Rationale for anti-GITR cancer immunotherapy. Eur J Cancer. 2016 Nov; 67: 1–10. Doi: 10.1016/j.ejca.2016.06.028. Epub 2016 Aug 31. PMID: 27591414. https://www.ejcancer.com/article/S0959-8049(16)32341-3/fulltext

Zappasodi R., Sirard C., Li Y., Budhu S., Abu-Akeel M., Liu C., Yang X., Zhong H., Newman W., Qi J., Wong P., Schaer D., Koon H., Velcheti V., Hellmann M. D., Postow M. A., Callahan M. K., Wolchok J. D., Merghoub T. Rational design of anti-GITR-based combination im-

munotherapy. Nat Med. 2019 May; 25(5): 759–766. Doi: 10.1038/s41591–019–0420–8. Epub 2019 Apr 29. PMID: 31036879; PMCID: PMC7457830. https://www.ncbi.nlm.nih.gov/pmc/articles/PMC7457830/pdf/nihms-1616665.pdf

Schöning-Stierand, K., Diedrich, K., Ehrt, C., Flachsenberg, F., Graef, J., Sieg, J., Penner, P., Poppinga, M., Ungethüm, A., Rarey, M. (2022). ProteinsPlus: a comprehensive collection of web-based molecular modeling tools. Nucleic Acids Research, – 50: W611-W615.

Kozakov D., Grove L. E., Hall D. R., Bohnuud T., Mottarella S. E., Luo L., Xia B., Beglov D., Vajda S. The FTMap family of web servers for determining and characterizing ligand-binding hot spots of proteins *Nature Protocols* 2015: 10(5): 733–755.

Ngan C. H., Hall D. R., Zerbe B. S., Grove L. E., Kozakov D., Vajda S. FTSite: high accuracy detection of ligand binding sites on unbound protein structures *Bioinformatics* 2012 28: 286–287.

Brenke R., Kozakov D., Chuang G. Y., Beglov D., Hall D., Landon M. R., Mattos C., Vajda S. Fragment-based identification of druggable 'hot spots' of proteins using Fourier domain correlation techniques. *Bioinformatics*. 2009. Mar 1.

Dávid Jakubec, Petr Škoda, Radoslav Krivák, Marian Novotný and David Hoksza. PrankWeb 3: accelerated ligand-binding site predictions for experimental and modelled protein structures. Nucleic Acids Research. May, 2022.

Lukáš Jendele and Radoslav Krivák and Petr Škoda and Marian Novotný and David Hoksza. PrankWeb: a web server for ligand binding site prediction and visualization. Nucleic Acids Research. May, 2019.

Radoslav Krivák and David Hoksza. P2Rank: machine learning based tool for rapid and accurate prediction of ligand binding sites from protein structure. Journal of Cheminformatics. Aug. 2018.

submitted 26.07.2025;
accepted for publication 10.08.2025;
published 31.10.2025

Contact: vishresh.deepak@gmail.com